

Supporting Information

Heteroaggregation of Virions and Microplastics Reduces the Number of Active Bacteriophages in Aqueous Environments

Enkhlin Ochirbat ^{1, ‡}, Rafał Zbonikowski ^{1, ‡}, Anna Sulicka ^{1,2}, Bartłomiej Bończak ¹,
Magdalena Bonarowska ¹, Marcin Łoś ^{3,4}, Elżbieta Malinowska ^{2,5}, Robert Hołyst ¹,
Jan Paczesny ^{1,*}

eoehirbat@ichf.edu.pl, rzbonikowski@ichf.edu.pl, anna.sulicka@o2.pl,
bbonczak@ichf.edu.pl, mbonarowska@ichf.edu.pl, mlos@biotech.ug.gda.pl,
elzbieta.malinowska@pw.edu.pl, rholyst@ichf.edu.pl, jpaczesny@ichf.edu.pl

Affiliations: ¹ Institute of Physical Chemistry, Polish Academy of Sciences, Kasprzaka 44/52,
01-224 Warsaw, Poland

² Warsaw University of Technology, Faculty of Chemistry, The Chair of Medical
Biotechnology, Noakowskiego 3, 00-664, Warsaw, Poland

³ Department of Molecular Biology, University of Gdansk, Wita Stwosza 59, 80-308 Gdansk,
Poland

⁴ Phage Consultants, Partyzantów 10/18, 80-254 Gdansk, Poland

⁵ Warsaw University of Technology, CEZAMAT, Poleczki 19, 02-822, Warsaw, Poland

* **Corresponding Author:** Jan Paczesny jpaczesny@ichf.edu.pl, +48 22 343 2071

22 **1. Materials and Methods**

23 **1.1. Chemicals**

24 LB-agar contained 15 g/L of agar, 10 g/L of NaCl, 10 g/L of tryptone, and 5 g/L of yeast extract
25 and was used as an instant mix (Carl Roth, Germany). LB-medium had the same composition
26 except for the lack of 15 g/L of agar (Carl Roth, Germany). TM buffer (pH=7.4) was prepared
27 using 10 mM Tris base, 5 μ M CaCl₂, 10 mM MgSO₄, and ultrapure water. All chemicals were
28 purchased from Sigma Aldrich (Germany). All solutions were sterilized by autoclaving
29 before use.

30 **1.1. Preparation of the bacteriophages**

31 Phages were obtained from Phage Consultants, Partyzantów, Gdańsk, Poland. An early
32 logarithmic culture of *Escherichia coli* BL21 was infected by T4. For MS2 and M13
33 multiplication, the *E. coli* C3000 strain was used. After lysis, T4 and M13 phages were
34 precipitated using polyethylene glycol. The precipitates of phages T4 and M13 were purified
35 by centrifugation and diluted with 1 M NaCl. Then CsCl gradient centrifugation was applied
36 (Beckman Optima XL70 ultracentrifuge, Ti50 rotor, 100000 g). T4 and M13 suspensions were
37 dialyzed against a series of TM buffers of decreasing ionic strength. Afterward, 0.2 μ g/mL
38 Viscolase (A&A Biotechnology) was added to samples with phages T4 and M13 to digest
39 residual DNA remaining in TM buffer after the procedure. In the case of MS2, the lysate was
40 only filtered using 0.22 μ m syringe filters.

41 **1.2. Evaluation of the number of active phages in the suspensions – double overlay** 42 **method**

43 A double overlay method and droplet plaque counting test were conducted to assess phage
44 activity and virulence. A solution containing 0.4 mL LB medium and 0.5% agar was mixed
45 with 200 μ l of refreshed *E.coli* bacteria. Depending on the phage type, they were *E. coli* BL21
46 (T4) or *E. coli* C3000 (MS2 and M13). The solution prepared in this way was poured onto a

47 previously prepared petri dish with LB-agar (LB medium and 1.5% agar). After the agar with
48 the bacteria solidified, at least eight droplets (5 μ l each) of each adequately diluted phage
49 suspension were deposited onto the plate. Subsequently, the plates were incubated at 37 °C for
50 24 h. After removing the plates from the incubator, the plaques were counted, and the
51 concentration of phages was calculated and expressed in PFU/mL (plaque-forming units).

52 Microplastic and leachable experiments were done in triplicates. At least eight technical
53 replicates (droplets) were used for each experimental run to calculate phage titers. Standard
54 deviation is used as an experimental error. The Student`s t-test was performed to evaluate
55 whether the observed differences were statistically significant. * p-value < 0.05; ** p-value <
56 0.01; *** p-value < 0.001.

57

58 **Table S1.** Comparison of physical characteristics of MS2, M13, and T4 bacteriophages.

	MS2	M13	T4
shape	icosahedral	filamentous	complex (tailed)
size	23 to 28 nm (Kuzmanovic et al., 2003)	880 x 5.5 nm (Moghimian et al., 2016)	115 x 85 nm capsid, 92 x 24 nm tail, 145 nm motile fibers (Leiman et al., 2010; Yap and Rossmann, 2014)
genetic material	ssRNA	ssDNA	dsDNA
genome size	3569 nucleotides	6407 nucleotides	168 903 bp
zeta potential at pH around 7	around -40 mV (Armanious et al., 2016)	-18 mV (Putra et al., 2019)	-26 mV (Hosseinidoust et al., 2011)
dipole moment	NA	NA	24 kD (200 kD when the fibers are extended) (Greve and Blok, 1975)

59

60 **1.4. Microplastic BET characterization**

61 Surface areas, total pore volumes, and average pore size of polymers were determined by
62 Micromeritics ASAP2020. The weight of the samples was ~0.3 g. Before measurements, the
63 samples were degassed in a vacuum at 343 K for 5 hours to clean their surface. The adsorption
64 process was carried out at a temperature of liquid nitrogen (77 K), and krypton was used as an
65 adsorbent instead of the commonly used nitrogen. For extremely low surface area samples
66 (which is what the polymers discussed in this paper are), the number of non-adsorbed gas
67 molecules at adsorption equilibrium can exceed the number of molecules adsorbed on the
68 sample, which will hamper the sample's accurate measurement of gas uptake. Because of this
69 effect, the typical surface area detection limit for N₂ physisorption at 77 K is assumed to be
70 about 1 m². This detection limit may be significantly reduced by using krypton adsorption
71 analysis at the same temperature that krypton is below its triple point and where its saturation
72 pressure is 2.32 mbar, i.e., ~430 times lower than p_{sat} of N₂. It follows that at any given relative
73 gas pressure, the absolute pressure of Kr is 430 times lower than that of N₂. This also means
74 that the density of Kr in the free space is proportionally lower, which leads to a significant
75 improvement in the detection limit for Kr. The surface area calculation was carried out
76 following the theory of Brunauer, Emmet, Teller (BET) as recommended by the IUPAC for
77 low surface substances (Thommes et al., 2015). The BET model was applied in the range of
78 p/p_0 from 0.05 to 0.30, and the resulting BET plots showed linearity (the measurements error
79 level was 5%).

80 **1.5. Microplastic size analysis based on optical microscopy pictures**

81 Radii of the plastic microparticles based on optical microscopy were calculated with
82 ImageJ 1.53t. Firstly, the pictures of microparticles were adjusted to have sufficient contrast
83 with the background, and any imperfections like light reflexes on the particle surface were
84 masked manually. Then, the areas of the plane projections were integrated, and the radii of the

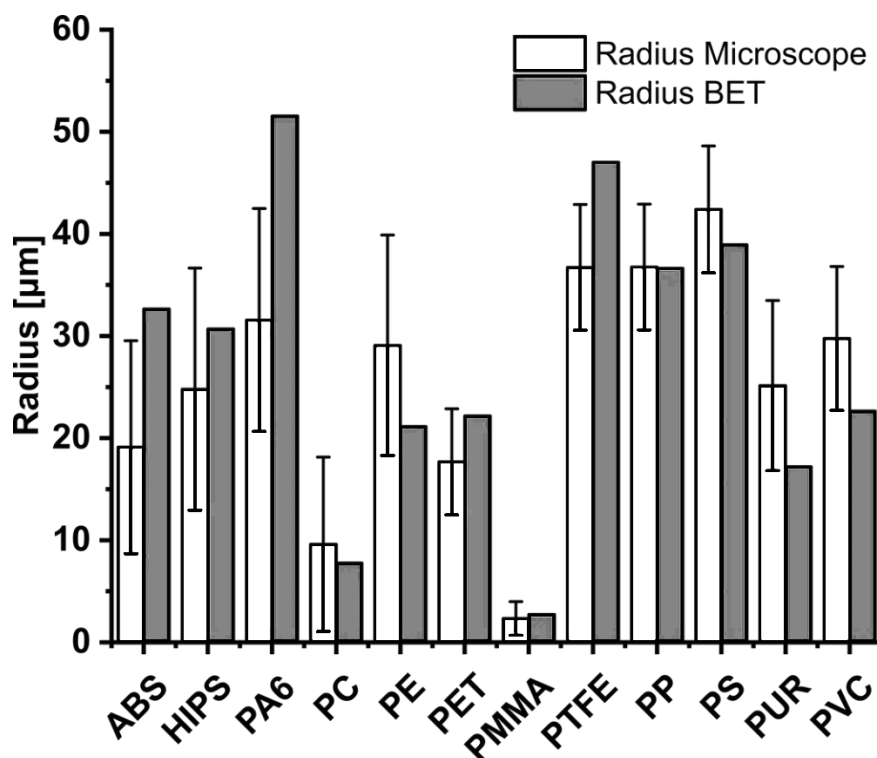
85 corresponding circles of the same area were calculated. Data is presented in **Table S2** and in
86 **Figure S1**.

87

88 **Table S2.** Sizes of particles calculated from images taken with a microscope (#1) and
89 calculated results from the BET measurement (#2).

Polymer	Radius (μm) #1 microscope	Radius (μm) #2 BET
ABS	19.12 ± 10.42	32.6
HIPS	24.80 ± 11.86	30.7
PA6	31.57 ± 10.92	51.6
PC	9.60 ± 8.55	7.8
PE	29.09 ± 10.80	21.1
PET	17.67 ± 5.20	22.2
PMMA	2.35 ± 1.65	2.7
PTFE	36.72 ± 6.17	47.0
PP	36.75 ± 6.16	36.6
PS	42.41 ± 6.20	38.9
PUR	25.15 ± 8.34	17.2
PVC	29.76 ± 7.05	22.6

90



91
 92 **Fig. S1.** Comparison of calculated radii size between direct measurement *via* microscope and
 93 BET measurement.

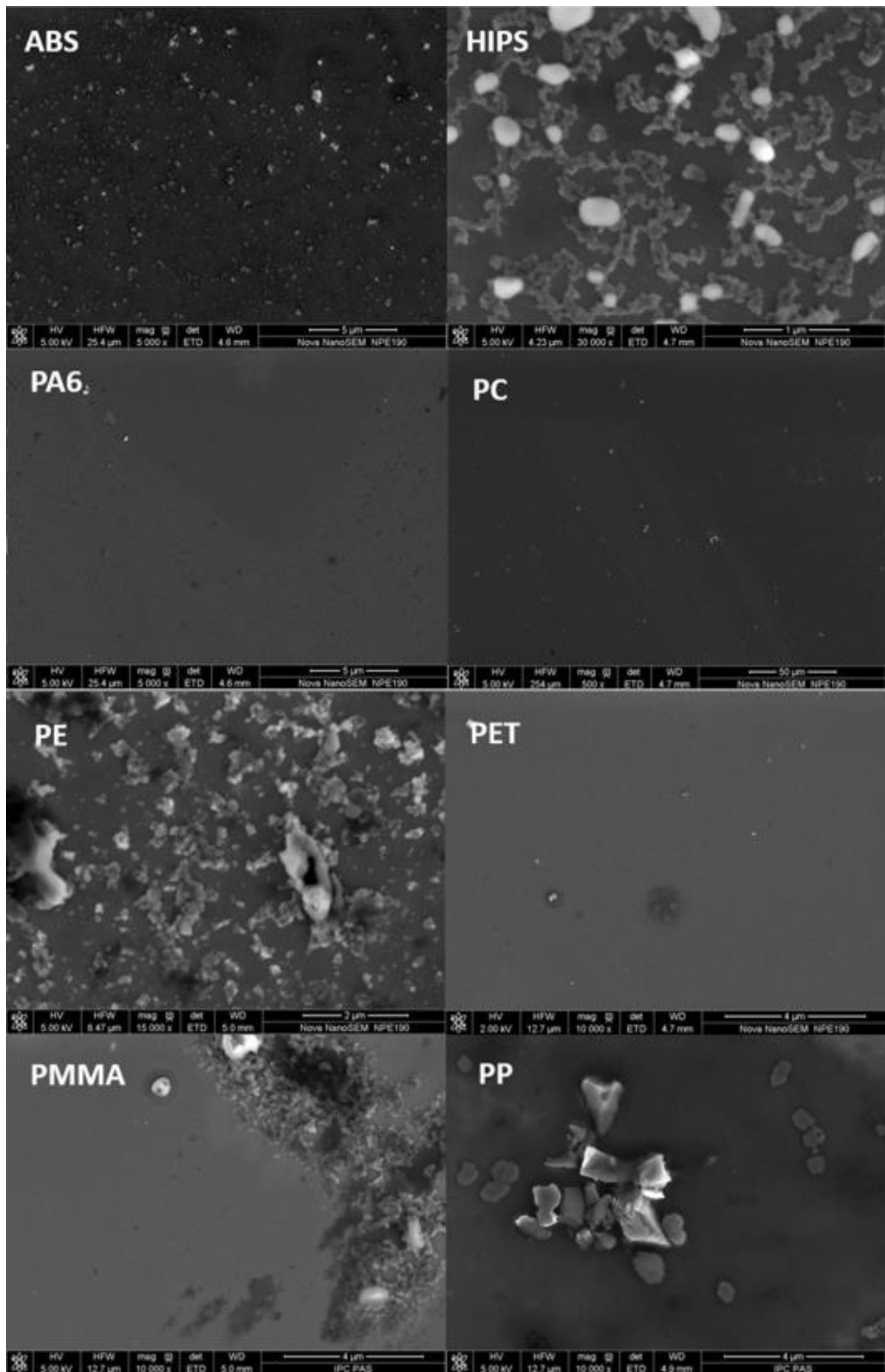
94 **1.6. Total organic carbon (TOC) measurement**

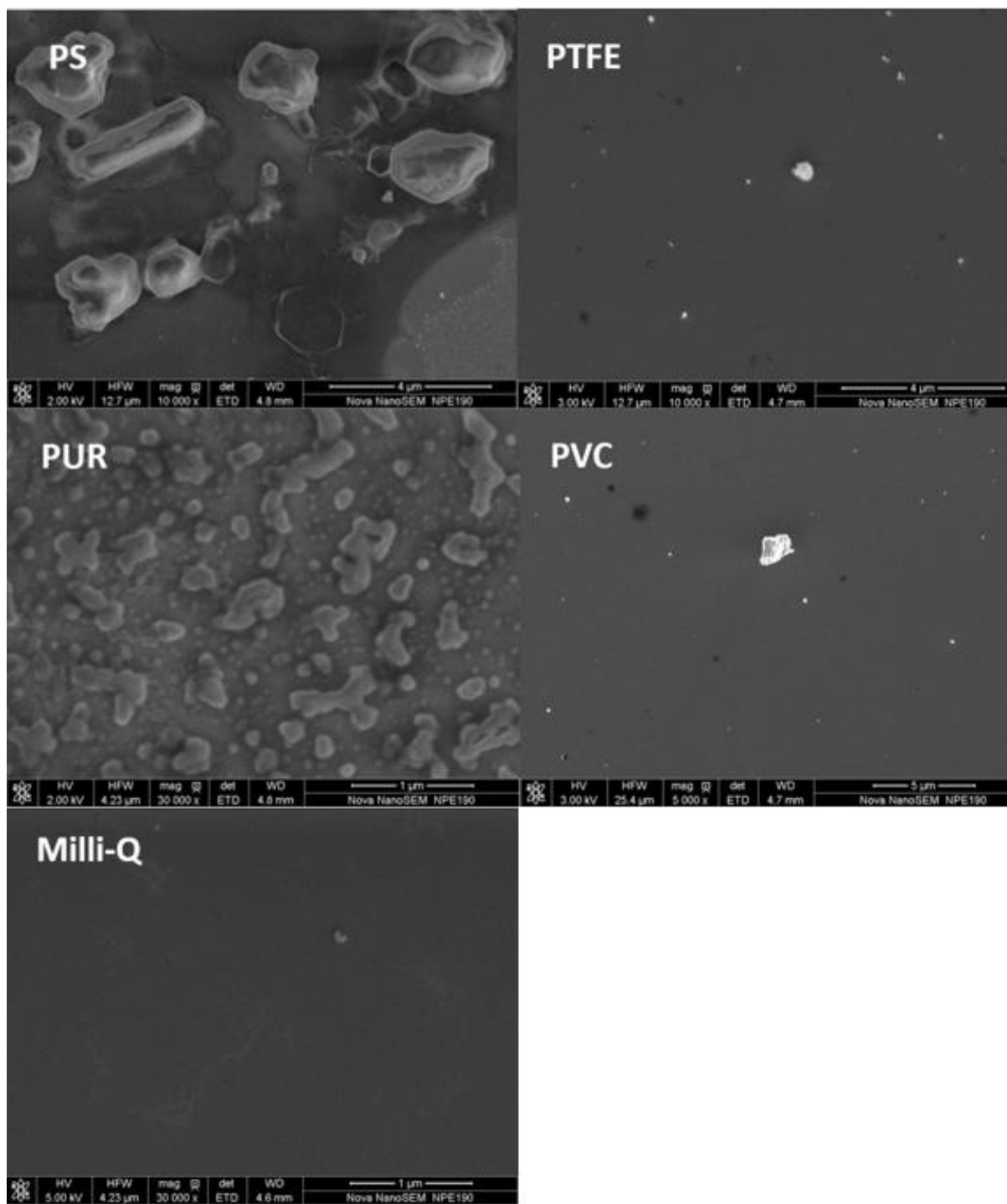
95 We prepared 40 mg samples of each polymer and soaked them in 40 mL of Milli-Q water for
 96 24 h (mixing). After filtration with a syringe filter (PES, 0.22 µm), resulted extracts were
 97 analyzed using Elementar – Vario EL III, CHNS to obtain total organic carbon. The results
 98 from all of the samples were below the detection limit (<0.03%) of the utilized instrument.
 99 Therefore, the analyzes were outsourced to a commercial and accredited laboratory (GBA
 100 POLSKA LLC). The measurements were done following the norm (PN-EN 1484:1999) with a
 101 lower detection limit (2 ppm). Only two samples, PA6 (4.5 ± 0.7 ppm) and PUR (3.5 ± 0.5
 102 ppm), gave results above the detection limit.

103 **1.7. SEM pictures taken from leachable samples.**

104 SEM pictures were taken (FEI Nova NanoSEM 450) to identify the sizes of particles solubilized
 105 in the leachable samples. We applied the leachables' suspensions on polished silica plates and

106 allowed them to dry out. A minimal number of objects were observed in PC, PET, PA6, PTFE,
107 and PVC cases. We found a moderate number of particles in the case of HIPS and PMMA. For
108 ABS, PP, PE, and PS samples, substantial quantities of particles equally distributed over the
109 silica plate were found. The SEM pictures shown in **Figure S2** showed that, at least in some
110 cases, microplastic fragmented further during the experiment into nano- and sub-microparticles.
111





113

114 **Figure S2.** SEM images demonstrating leachable and/or nanoparticles derived from filtered
 115 samples incubated with microplastics.

116

117

118 **2. Analysis of the results using the Classical Linear Regression Model** (Mycielski, 2010)

119 The **database** used for the analysis is provided as a separate file in the Supporting Information

120 (accudynetest.com access: 12.04.22; polymerdatabase.com access: 12.04.22; Kolska et al.

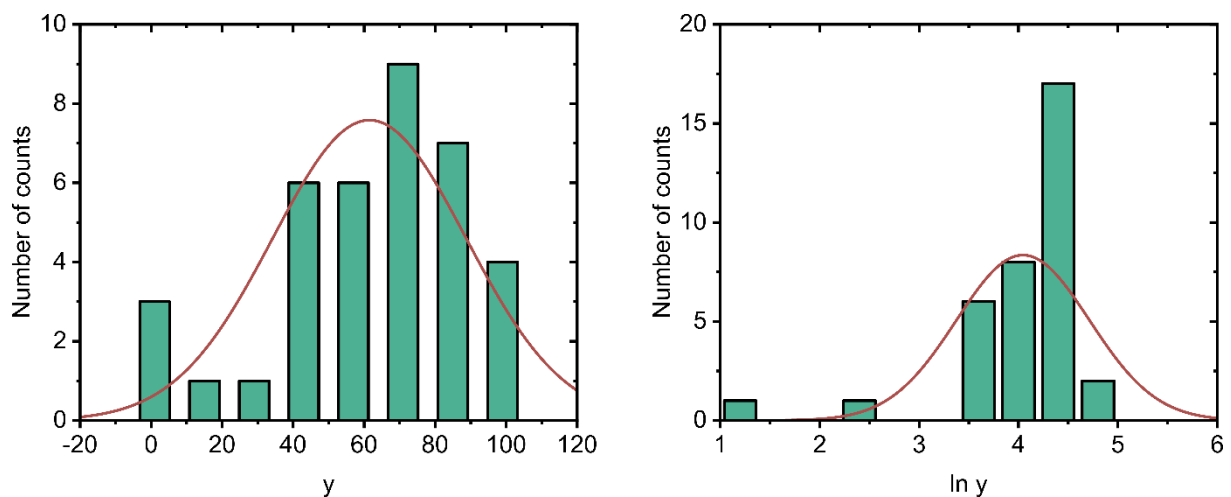
121 2013);(Hosseinioust et al., 2011; Armanious et al., 2016; Putra et al., 2019).

122 We adjusted the numbering of the equations in the Supporting information to match the
123 main text.

124 The dependent variable y_i was reserved for the percentage rate of phage titer after 24 h,
125 and taken as the mean value of three repetitions (*cf.* **Table 1** in the main text). To facilitate the
126 interpretation and increase the quality of the regression, an additional observation was added to
127 the database - $y_0 = 100\%$ for all the explanatory variables equal to 0.

128 At the initial state of modeling, we compared the distribution of y and $\ln y$ with the
129 fitted normal distribution (bins = 10) (**Figure S3**). Based on the observations and a few initial
130 regressions, we decided not to use a logarithmic variable for further analysis.

131



132

133 **Figure S3.** Histograms of the possible functional form of the explained variable and its normal
134 distribution fit (left – y , right – $\ln y$).

135

136 Among the explanatory variables were:

- 137 • Zeta potential of the polymer (*zeta*), the contact angle of the polymer found in the literature
138 (*conangle*), the measured wetting angle (*wetangle*), the results of the BET measurement
139 (*bet*), the density of the polymer (*density*), the influence of the leachables measured as a
140 percentage drop from **Table 1** (main text) (*leachable*);
- 141 • Functions of continuous variables, for instance, $\text{coswetangle} = \cos(\text{wetangle})$, $\text{zeta2} = \text{zeta}^2$,
142 $\tanh(a \text{ zeta})$, where *a* is a parameter between 0.00001 to 0.100000;
- 143 • Categorical variables concerning bacteriophage like (*t4*, *ms2*, *m13*), used polymer (*abs*, *hips*,
144 *pa6*, *pc*, *pe*, *pet*, *pmma*, *pp*, *ps*, *ptfe*, *pur*, *pvc*);
- 145 • Binary variables like *color* (if the color of the polymer is not white, indicating the addition
146 of specific dyes), *hydrophob* (if the wetting angle of the polymer was higher than 90 °);
- 147 • Interactions of variables and functions of those interactions, for example,
148 $\text{int_t4_zeta} = \text{t4} \cdot \text{zeta}$ presenting the value of zeta potential of the polymer if the used phage
149 was T4, unless it returns 0.

150 All the used variables with the description can be found in the database.

151 **2.1. Coarse estimation**

152 The coarse estimation for categorical variables was conducted. The variables describing the
153 bacteriophage and the polymer were divided into binary variables (*ms2*, *m13*, *abs*, *hips*, *pa6*,
154 *pc*, *pe*, *pet*, *pmma*, *pp*, *ps*, *ptfe*, *pur*, *pvc*). Variable *pp* = 1 was taken as the base level.

Source	SS	df	MS	Number of obs	=	37
Model	21079.1708	14	1505.65506	F(14, 22)	=	6.43
Residual	5154.40675	22	234.291216	Prob > F	=	0.0001
				R-squared	=	0.8035
				Adj R-squared	=	0.6785
Total	26233.5775	36	728.710487	Root MSE	=	15.307

y	Coefficient	Std. err.	t	P> t	[95% conf. interval]	
t4	-25.59583	18.03897	-1.42	0.170	-63.00637	11.8147
ms2	-32.055	18.03897	-1.78	0.089	-69.46554	5.355536
m13	-45.50917	18.03897	-2.52	0.019	-82.9197	-8.098631
abs	-17.65333	12.49777	-1.41	0.172	-43.57211	8.265446
hips	6.949999	12.49777	0.56	0.584	-18.96878	32.86878
pa6	11.87	12.49777	0.95	0.353	-14.04878	37.78878
pc	13.19	12.49777	1.06	0.303	-12.72878	39.10878
pe	13.59667	12.49777	1.09	0.288	-12.32211	39.51545
pet	-50.42	12.49777	-4.03	0.001	-76.33878	-24.50122
pmma	12.66	12.49777	1.01	0.322	-13.25878	38.57878
pp	0	(omitted)				
ps	-20.79	12.49777	-1.66	0.110	-46.70878	5.12878
ptfe	14.92333	12.49777	1.19	0.245	-10.99545	40.84211
pur	-10.27333	12.49777	-0.82	0.420	-36.19211	15.64545
pvc	-41.71333	12.49777	-3.34	0.003	-67.63211	-15.79455
_cons	100	15.30657	6.53	0.000	68.25611	131.7439

155

156 The estimation showed that separate effects of replacing a particular polymer and
 157 choosing the bacteriophage could describe the variance of the investigated phenomenon in
 158 almost 80%. However, the estimated parameters had a relatively high standard error.

159 The regression with only the type of the polymer (and not phage type) revealed the
 160 average decrease in the activity of phages due to a specific polymer. R^2 dropped from around
 161 0.80 (polymers and phages) to around 0.71 (only polymers).

Source	SS	df	MS	Number of obs	=	37
Model	18602.0657	12	1550.17214	F(12, 24)	=	4.88
Residual	7631.51184	24	317.97966	Prob > F	=	0.0005
				R-squared	=	0.7091
				Adj R-squared	=	0.5636
Total	26233.5775	36	728.710487	Root MSE	=	17.832

y	Coefficient	Std. err.	t	P> t	[95% conf. interval]	
abs	-52.04	20.5906	-2.53	0.018	-94.53691	-9.543086
hips	-27.43667	20.5906	-1.33	0.195	-69.93358	15.06025
pa6	-22.51667	20.5906	-1.09	0.285	-65.01358	19.98025
pc	-21.19667	20.5906	-1.03	0.314	-63.69358	21.30025
pe	-20.79	20.5906	-1.01	0.323	-63.28691	21.70691
pet	-84.80667	20.5906	-4.12	0.000	-127.3036	-42.30975
pma	-21.72667	20.5906	-1.06	0.302	-64.22358	20.77025
pp	-34.38667	20.5906	-1.67	0.108	-76.88358	8.110247
ps	-55.17667	20.5906	-2.68	0.013	-97.67358	-12.67975
ptfe	-19.46333	20.5906	-0.95	0.354	-61.96025	23.03358
pur	-44.66	20.5906	-2.17	0.040	-87.15691	-2.163087
pvc	-76.1	20.5906	-3.70	0.001	-118.5969	-33.60309
_cons	100	17.83198	5.61	0.000	63.19659	136.8034

162

163 2.2. Building the model

164 The standard protocol is to start building a model by eliminating irrelevant variables. However,
 165 in our case, having a limited number of observations, we decided to do it from the bottom by
 166 trial and error. We replaced categorical variables with physicochemical variables related to
 167 adsorption, thermodynamics, heteroaggregation, and the physical chemistry of colloids.

168 The raw data revealed a relatively weak linear dependence of y on ζ .

Source	SS	df	MS	Number of obs	=	37
Model	3048.96832	1	3048.96832	F(1, 35)	=	4.60
Residual	23184.6092	35	662.417406	Prob > F	=	0.0389
				R-squared	=	0.1162
				Adj R-squared	=	0.0910
Total	26233.5775	36	728.710487	Root MSE	=	25.737

y	Coefficient	Std. err.	t	P> t	[95% conf. interval]	
zeta	.6259195	.291748	2.15	0.039	.0336396	1.218199
_cons	91.17702	14.66314	6.22	0.000	61.40927	120.9448

169

170 According to the DLVO theory (Derjaguin et al., 1987; Ohshima, 2012), describing the
 171 stability of identical spheres (colloid), interaction energy can be defined as a sum of the van der

172 Waals attraction energy and double layer repulsion energy. Repulsion free energy of two
 173 spheres can be described as:

$$174 \quad E = \frac{64\pi k_B T R \rho_\infty \gamma^2}{\kappa^2} e^{-\kappa d} \quad (3)$$

$$175 \quad \gamma = \tanh\left(\frac{ze_0\psi_0}{4k_B T}\right) \quad (4)$$

176 where, R – radius of the sphere, ρ_∞ - the number density of ions in the bulk solution, γ – reduced
 177 surface potential, d – the distance between spheres, z – valency of the ion. We assumed that
 178 based on this theory, we have to sort the *zeta* variable and couple it with the bacteriophage type.
 179 Various phages have very different physicochemical properties (*cf.* **Table S2**). Thus, we
 180 introduced interactions between the phage type and the polymer's zeta potential. Then, by the
 181 simple estimation, we proposed that the reduced surface potential should depend on zeta
 182 potential ζ as described:

$$183 \quad \gamma = \tanh(a\zeta) \quad (7)$$

$$184 \quad a \in [0.00001, 0.10000]$$

185 Because the energy of the repulsion depends on γ^2 (equation 3) we assumed that the
 186 best linear regression was reached (the highest R^2) for the lowest a , when the R^2 reached the
 187 same value as for the squared interaction of polymer zeta potential and the phage type. Hence,
 188 to simplify the model, we decided to include interactions of phage and squared zeta potential
 189 of the polymer (*int_t4_zeta2*, *int_ms2_zeta2*, *int_m13_zeta2*).

Source	SS	df	MS	Number of obs	=	37
Model	6630.62157	3	2210.20719	F(3, 33)	=	3.72
Residual	19602.956	33	594.028969	Prob > F	=	0.0208
				R-squared	=	0.2528
				Adj R-squared	=	0.1848
Total	26233.5775	36	728.710487	Root MSE	=	24.373
y	Coefficient	Std. err.	t	P> t	[95% conf. interval]	
int_t4_zeta2	-.0020935	.0031583	-0.66	0.512	-.0085191	.0043321
int_ms2_zeta2	-.0058698	.0031583	-1.86	0.072	-.0122954	.0005558
int_m13_zeta2	-.009881	.0031583	-3.13	0.004	-.0163066	-.0034554
_cons	76.08184	7.52908	10.11	0.000	60.76381	91.39986

190

191 The variable *int_t4_zeta2* was excluded from the further analysis as the value of the
192 coefficient oscillated around 0 with a high standard error. P-value showed that we could not say
193 if this parameter is not equal to zero on any rational significance level (neither 0.05 nor 0.10).

194 We assumed the hydrophobicity of the polymer as an essential variable describing the
195 phenomenon. However, we did not get satisfying results by introducing variables like wetting
196 angle, trigonometrical functions of wetting angle, contact angle, binary segregation of polymer
197 based on the condition $\theta > 90^\circ$, and other derivatives. We concluded that a better variable might
198 be related to the work of adhesion (the work needed to separate a unit of area of two phases)
199 described by the Young-Dupré equation, where σ – surface tension of the liquid (Schrader,
200 1995):

$$201 \quad W = \sigma(1 + \cos \theta) \quad (8)$$

202 The total work is proportional to the area. Therefore, we introduced the new variable

$$203 \quad betcoswet = (bet + bet \cos(wetangle)) \quad (9)$$

204 This still did not improve the model. Similar variables (for instance, *langmuircoswet*),
205 which were tested, are described in the database.

206 Further analysis revealed significant improvements in the model quality by using the
207 *radius* being a calculated radius of an average plastic particle according to the equation:

$$208 \quad r (\mu m) = \frac{3}{bet \cdot density} \quad (6)$$

209 The best outcomes were found when *radius* and *radius2* ($radius^2$) were used simultaneously
210 (i.e., the dependence on r was nonlinear). Other similar variables which were tested are
211 described in the database.

212 These preliminary findings brought us to a few potential models depending on the
213 approach towards the analysis: **Model 1A** and **Model 1B**, and **Model 2**.

214 **Model 1A** and **1B** are entirely based on physicochemical data. This analysis omitted
215 PUR, because this polymer might be produced with different monomers and additives.
216 Literature data for PUR varies so much that we decided to omit the polymer from the model.

217 **Model 2** was created by looking for a physicochemical parameter that could describe
218 most of the results of the experiments. The other physicochemical properties were included in
219 categorical variables of a particular polymer and removed from the regression if their impact
220 was not significant (significance level 0.05). This approach assumed that few parameters would
221 govern the phenomenon and are not neglectable. At the same time, modeling allowed for some
222 polymers to have specific features, which caused inconsistency with the rest of the results.

223

224 **2.3. Model 1A**

225 This approach combined variables related to zeta potential squared concerning the specific
 226 phage, the radius of the particles in nonlinear form ($\beta_i r + \beta_j r^2$) and cosine of contact angle.

Source	SS	df	MS	Number of obs	=	34
Model	16969.1009	6	2828.18349	F(6, 27)	=	8.53
Residual	8948.00001	27	331.407408	Prob > F	=	0.0000
				R-squared	=	0.6547
				Adj R-squared	=	0.5780
Total	25917.101	33	785.366696	Root MSE	=	18.205

y	Coefficient	Std. err.	t	P> t	[95% conf. interval]	
int_t4_zeta2	-.0009271	.0025219	-0.37	0.716	-.0061016	.0042475
int_ms2_zeta2	-.0045919	.0025219	-1.82	0.080	-.0097664	.0005827
int_m13_zeta2	-.0087035	.0025219	-3.45	0.002	-.013878	-.0035289
radius	-3.368492	.7750578	-4.35	0.000	-4.958779	-1.778205
radius2	.0520132	.0142139	3.66	0.001	.0228487	.0811776
cosconangle	-81.8548	19.71571	-4.15	0.000	-122.3081	-41.40149
_cons	119.0144	10.8045	11.02	0.000	96.84541	141.1834

227

228 ***F*-statistic, R^2 , adjusted R^2**

229 As the F-statistic is equal to 8.53 and the p-value ≈ 0.0000 , we can conclude that there is a
 230 statistically significant relationship between y and the chosen explanatory variables. 65.47% of
 231 the variance of y is explained by the selected explanatory variables. The adjusted R^2 (correcting
 232 the positive bias related to the number of observations and number of explanatory variables)
 233 shows that the model should explain 57.80% of the variance of y in the population.

234 ***Ramsey RESET test***

Ramsey RESET test for omitted variables

Omitted: Powers of fitted values of y

H0: Model has no omitted variables

F(3, 24) = 3.30

Prob > F = 0.0377

235

236 With the p-value of 0.0377, we reject the hypothesis of the correct specification of the model
 237 (significance level of 0.05). However, in our analysis, we suspected that the model's linear form
 238 might not be sufficient when all qualitative (categorical or binary) variables were excluded from

239 the model. A similar model, neglecting *int_t4_zeta2* and *int_t4_zeta2*, passed the RESET test.
 240 Nonetheless, we decided to keep those variables.

241 On the significance level of 0.05, we failed to reject the hypothesis that the estimated
 242 parameters of variables *int_m13_zeta2*, *cosconangle*, *radius*, and *radius2* are equal to zero. For
 243 *int_ms2_zeta2* we fail to reject the same hypothesis on the significance level = 0.10.
 244 *int_t4_zeta2* was kept in the model for the reason described in the previous paragraph.

245 **Correlation Matrix**

246 As suspected, there is high collinearity between variables *radius* and *radius2*, but not other
 247 variables.

	int_t4~2	int_ms~2	int_m1~2	radius	radius2	coscon~e
int_t4_zeta2	1.0000					
int_ms2_ze~2	-0.3042	1.0000				
int_m13_ze~2	-0.3042	-0.3042	1.0000			
radius	-0.0188	-0.0188	-0.0188	1.0000		
radius2	-0.0555	-0.0555	-0.0555	0.9577	1.0000	
cosconangle	-0.0447	-0.0447	-0.0447	-0.5215	-0.4895	1.0000

249 **Multicollinearity**

250 Again, as expected *radius* and *radius2* present high VIF values, but they were introduced to the
 251 model on purpose. VIF values for other variables are much lower than 10.

Variable	VIF	1/VIF
radius2	13.91	0.071878
radius	13.90	0.071924
int_m13_ze~2	1.52	0.656327
int_ms2_ze~2	1.52	0.656327
int_t4_zeta2	1.52	0.656327
cosconangle	1.42	0.704801
Mean VIF	5.63	

253 **Residuals analysis and homoskedasticity**

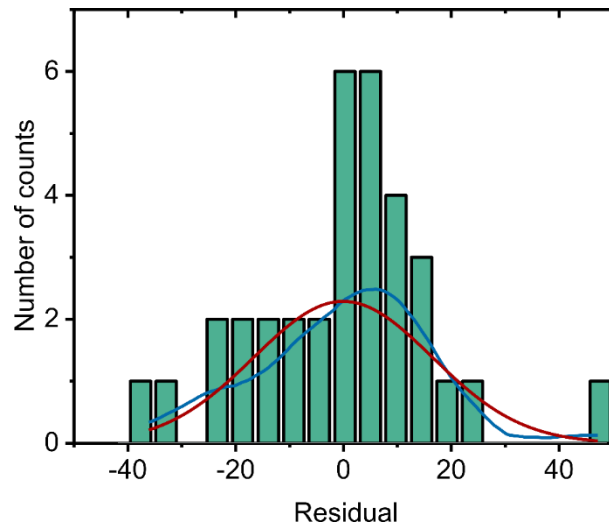
254 According to the Shapiro-Wilk test, we fail to reject the 0-hypothesis of the normal distribution
 255 of residuals in the model at the significance level of 0.05 (p-value = 0.26195). The distribution
 256 is presented in **Figure S4**. The Kernel density plot (normalized to the number of counts) almost

257 matches the Gaussian curve. There was no strong skewness, nor was kurtosis noticed (too few
 258 observations may cause it).

Shapiro-Wilk W test for normal data

Variable	Obs	W	V	z	Prob>z
e	34	0.96111	1.358	0.637	0.26195

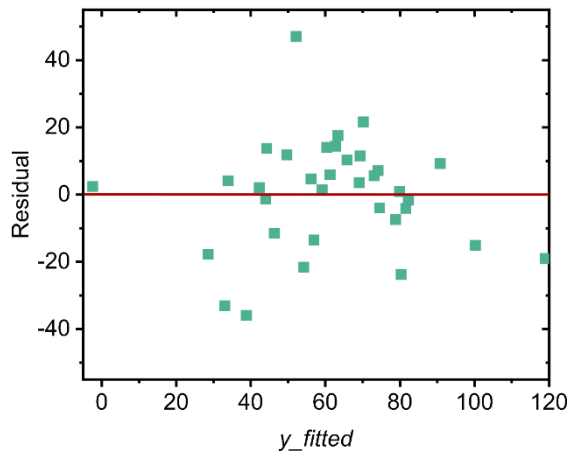
259
 260



261
 262
 263
 264

Figure S4. The histogram of the residuals of the model. Blue curve – Kernel density normalized to the number of counts, red curve – normal distribution.

265 According to the Breusch-Pagan test, we fail to reject the hypothesis of constant
 266 variance (homoskedasticity) at the significance level of 0.05. The same conclusion was received
 267 from White’s test. At the same significance level, we also fail to reject the hypothesis of
 268 skewness and kurtosis of the distribution of residuals (**Figure S5**).



269

270 **Figure S5.** Residuals of the model for fitted values of y_i .

271

Breusch-Pagan/Cook-Weisberg test for heteroskedasticity
 Assumption: Normal error terms
 Variable: Fitted values of y

H0: Constant variance

chi2(1) = 1.18
 Prob > chi2 = 0.2767

272

White's test
 H0: Homoskedasticity
 Ha: Unrestricted heteroskedasticity

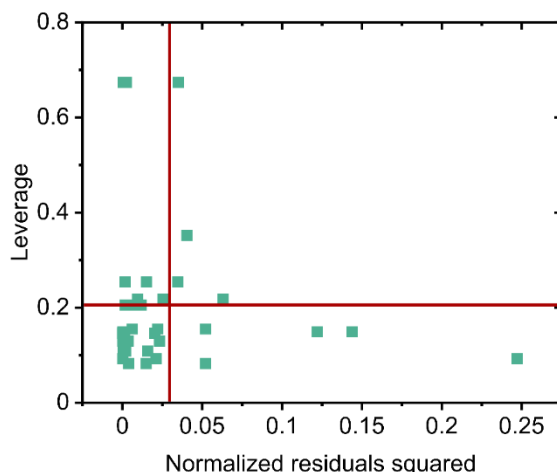
chi2(21) = 21.22
 Prob > chi2 = 0.4457

Cameron & Trivedi's decomposition of IM-test

Source	chi2	df	p
Heteroskedasticity	21.22	21	0.4457
Skewness	2.10	6	0.9103
Kurtosis	1.12	1	0.2889
Total	24.44	28	0.6580

273

274 No observations should be removed from the model because none of them was spotted
 275 in the leverage-normalized residual squared plot's upper-right corner (**Figure S6**). In other
 276 words, no observation strongly biases the estimated β -coefficients.



277

278 **Figure S6.** The leverages-normalized residual squared analysis.

279

280 *Interpretation of the model*

281 The model did not pass the RESET, but passed the other tests according to the diagnostics.

282 However, it is essential to mention that the model was based only on 36 experiments (each

283 experiment consisted of 3 repetitions of 8 repetitions of the phage titration) and an additional

284 theoretical observation (base 100% activity of the certain bacteriophage after 24 h if any

285 polymer was added). Due to so few observations, the model may omit some important

286 information, even if the statistical analysis based on the available data is valid. This issue is also

287 visible in high standard errors of the parameters.

288 The final form of the model assumed independent variables and their impact on the

289 explained variable y_i (i.e., the activity of the bacteriophage after 24 h [%]):

$$290 \quad y_i = \beta_0 + \beta_1 \cdot \text{int_t4_zeta2} + \beta_2 \cdot \text{int_ms2_zeta2} + \beta_3 \cdot \text{int_m13_zeta2} + \beta_4 \cdot \text{radius} +$$

$$291 \quad \beta_5 \cdot \text{radius2} + \beta_6 \cdot \text{coscotangle} \quad (10)$$

292 60.75% of the variance of y is explained by the chosen explanatory variables. The

293 adjusted R^2 (correcting the positive bias related to the number of observations and number of

294 explanatory variables) shows that the model should explain 55.33% of the variance of y in the

295 population. The model's estimated parameters (coefficients) are given in **Table S3**.

296 **Table S3.** Estimated parameters (coefficients) of the model.

Estimated parameter	Value	Standard Error	Unit
β_0	119.0145	10.80451	-
β_1	-0.0009271	0.0025219	mV ⁻²
β_2	-0.0045919	0.0025219	mV ⁻²
β_3	-0.0087035	0.0025219	mV ⁻²
β_4	-3.368489	0.7750576	μm^{-1}
β_5	0.052013	0.0142138	μm^{-2}
β_6	-81.855	19.71572	-

297

298 - The constant value $\beta_0 = 119.0145 \pm 10.80451$ represents the basic level, theoretically
 299 100% activity of the certain bacteriophage.

300 - For T4 bacteriophage, the activity drops 0.0009271 ± 0.0025219 pp with the increase of
 301 1 mV² of the squared zeta potential of the polymer.

302 - For MS2 bacteriophage, the activity drops 0.0045919 ± 0.0025219 pp with the increase
 303 of 1 mV² of the squared zeta potential of the polymer.

304 - For M13 bacteriophage, the activity drops 0.0087035 ± 0.0025219 pp with the increase
 305 of 1 mV² of the squared zeta potential of the polymer.

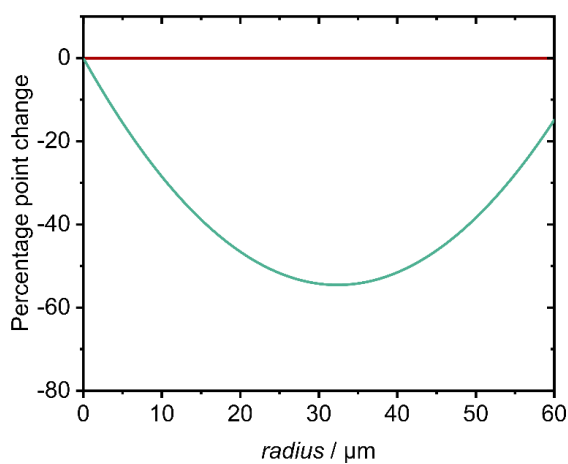
306 - The activity drops 3.368489 ± 0.7750576 pp with the increase of 1 μm of the average
 307 radius of the plastic microparticle.

308 - The activity rises 0.052013 ± 0.0142138 pp with the increase of 1 μm^2 of the average
 309 squared radius of the plastic microparticle.

310 - The activity drops 81.855 ± 19.71572 pp for the *coscotangle* = 1

311

312 The variable *radius* depends on two variables *bet* (the surface area of the polymer measured
313 with BET method [$\text{m}^2 \cdot \text{g}^{-1}$]) and *density* (the density of the polymer [$\text{g}^2 \cdot \text{cm}^{-3}$]) according to
314 equation 6. The change of fitted value y_i depending on the *radius* is presented in **Figure S7**.
315 Both very small and very large particles are not efficient in scavenging phages.



316
317 **Figure S7.** Change of the fitted y_i depending on the radius of the plastic microparticle.
318

319 **2.4. Model 1B**

320 **Model 1B** is modified **Model 1A**, i.e., without two variables: *int_t4_zeta2* and *int_ms2_zeta2*.

321 They were removed because of too high a statistical probability that the β coefficients are equal

322 to zero.

Source	SS	df	MS	Number of obs	=	34
Model	15743.6002	4	3935.90004	F(4, 29)	=	11.22
Residual	10173.5008	29	350.810372	Prob > F	=	0.0000
				R-squared	=	0.6075
				Adj R-squared	=	0.5533
Total	25917.101	33	785.366696	Root MSE	=	18.73

y	Coefficient	Std. err.	t	P> t	[95% conf. interval]
int_m13_zeta2	-.0068718	.0021243	-3.23	0.003	-.0112164 -.0025272
radius	-3.646578	.7646678	-4.77	0.000	-5.210499 -2.082656
radius2	.0581181	.013755	4.23	0.000	.0299859 .0862504
cosconangle	-77.76235	20.00964	-3.89	0.001	-118.6866 -36.83805
_cons	114.2707	10.42509	10.96	0.000	92.94901 135.5924

323

324 ***F*-statistic, R^2 , adjusted R^2**

325 As the *F*-statistic is equal to 11.22 and the *p*-value ≈ 0.0000 , we can conclude that there is a

326 statistically significant relationship between *y* and the chosen explanatory variables. 60.75% of

327 the variance of *y* is explained by the chosen explanatory variables. The adjusted R^2 (correcting

328 the positive bias related to the number of observations and number of explanatory variables)

329 shows that the model should explain 55.33% of the variance of *y* in the population.

330 ***Ramsey RESET test***

Ramsey RESET test for omitted variables

Omitted: Powers of fitted values of *y*

H0: Model has no omitted variables

F(3, 26) = 0.86

Prob > F = 0.4744

331

332 With the *p*-value of 0.4744, we fail to reject the hypothesis of the correct specification of the

333 model (significance level of 0.05). On the significance level of 0.05, we fail to reject the

334 hypothesis that the estimated parameters of variables *int_m13_zeta2*, *cosconangle*, *radius*, and
 335 *radius2* are equal to zero.

336 **Correlation Matrix**

337 There is high collinearity between variables *radius* and *radius2*, because $radius2 = radius^2$.

	int_m1~2	radius	radius2	coscon~e
int_m13_ze~2	1.0000			
radius	-0.0188	1.0000		
radius2	-0.0555	0.9577	1.0000	
cosconangle	-0.0447	-0.5215	-0.4895	1.0000

338
339

340 **Multicollinearity**

341 As expected *radius* and *radius2* present high VIF values, but they were introduced to the model
 342 on purpose. VIF values for other variables are much lower than 10.

Variable	VIF	1/VIF
radius	12.78	0.078218
radius2	12.31	0.081247
cosconangle	1.38	0.724308
int_m13_ze~2	1.02	0.979193
Mean VIF	6.87	

343

344 **Residuals analysis and homoskedasticity**

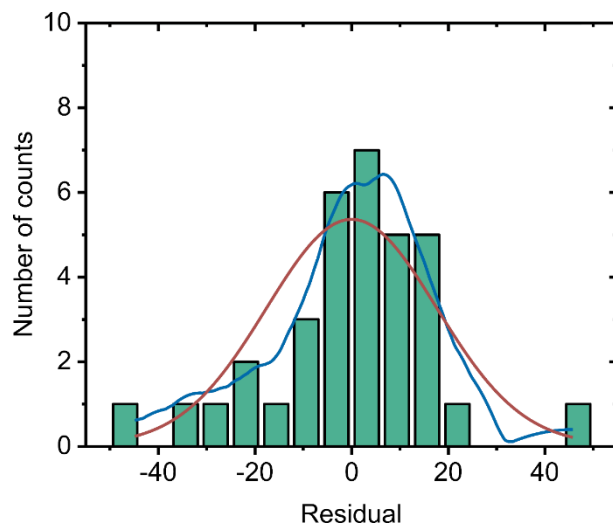
345 According to the Shapiro-Wilk test, we fail to reject the 0-hypothesis of the normal distribution
 346 of residuals in the model at the significance level of 0.05 (p-value = 0.14477). The distribution
 347 is presented in **Figure S8**. The Kernel density plot (normalized to the number of counts) almost
 348 matches the Gaussian curve. There was no strong skewness, nor was kurtosis noticed (too few
 349 observations may cause it).

Shapiro-Wilk W test for normal data

Variable	Obs	W	V	z	Prob>z
e	34	0.95239	1.662	1.059	0.14477

350

351

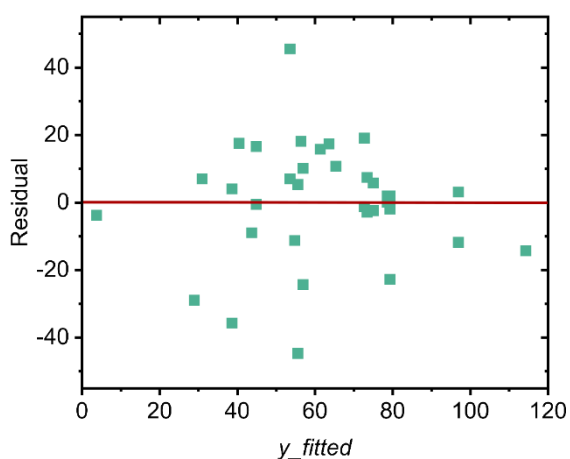


352

353 **Figure S8.** The histogram of the residuals of the model. Blue curve – Kernel density normalized
354 to the number of counts, red curve – normal distribution.

355

356 According to the Breusch-Pagan test, we fail to reject the hypothesis of constant
357 variance (homoskedasticity) at the significance level of 0.05. The same conclusion was received
358 from White's test. At the same significance level, we also fail to reject the hypothesis of
359 skewness and kurtosis of the distribution of residuals (**Figure S9**).



360

361 **Figure S9.** Residuals of the model for fitted values of y_i .

Breusch-Pagan/Cook-Weisberg test for heteroskedasticity
 Assumption: Normal error terms
 Variable: Fitted values of y

H0: Constant variance

chi2(1) = 2.01
 Prob > chi2 = 0.1568

362

White's test

H0: Homoskedasticity
 Ha: Unrestricted heteroskedasticity

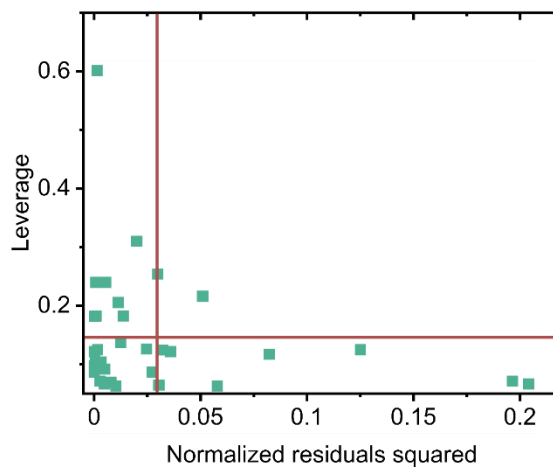
chi2(13) = 11.54
 Prob > chi2 = 0.5658

Cameron & Trivedi's decomposition of IM-test

Source	chi2	df	p
Heteroskedasticity	11.54	13	0.5658
Skewness	1.89	4	0.7561
Kurtosis	2.47	1	0.1159
Total	15.90	18	0.5996

363

364 No observations should be removed from the model because none of them was spotted
 365 in the leverage-normalized residual squared plot's upper-right corner (**Figure S10**). In other
 366 words, there is no observation that strongly bios the estimated β -coefficients.



367

368 **Figure S10.** The leverages-normalized residual squared analysis.

369

370

371

372 ***Interpretation of the model***

373 According to the diagnostics, the model seems to be valid for drawing nonbiased conclusions
 374 on the described phenomenon. However, it is important to mention that the model was based
 375 only on 36 experiments (each experiment consisted of 3 repetitions of 8 repetitions of the phage
 376 titration) and the additional theoretical observation (base 100% activity of the specific
 377 bacteriophage after 24 h if any polymer was added). Due to so few observations, the model may
 378 omit some important information, even if the statistical analysis based on the available data is
 379 valid. This issue is also visible in relatively high standard errors of the estimated parameters.

380 The final form of the model assumes independent variables and their impact on the
 381 explained variable y_i (the activity of the bacteriophage after 24 h [%]):

$$382 \quad y_i = \beta_0 + \beta_1 \cdot \text{int_m13_zetasqr} + \beta_2 \cdot \text{radius} + \beta_3 \cdot \text{radius2} + \beta_4 \cdot \text{coscotangle}$$

383 (11)

384 60.75% of the variance of y is explained by the chosen explanatory variables. The
 385 adjusted R^2 (correcting the positive bias related to the number of observations and number of
 386 explanatory variables) shows that the model should explain 55.33% of the variance of y in the
 387 population. The model's estimated parameters (coefficients) are given in **Table S4**.

388

389 **Table S4.** Estimated parameters (coefficients) of the model.

Estimated parameter	Value	Standard Error	Unit
β_0	114.2707	10.42509	-
β_1	-0.0068718	0.0021243	mV ⁻²
β_2	-3.646578	0.7646678	μm ⁻¹
β_3	0.0581181	0.013755	μm ⁻²
β_4	-77.76235	20.00964	-

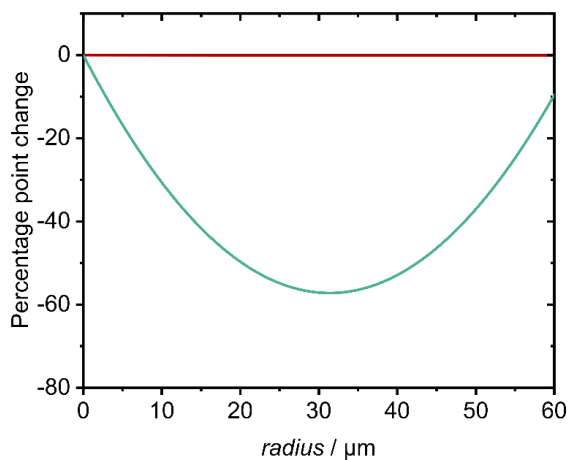
390

- 391 - The constant value $\beta_0 = 114.2707 \pm 10.42509$ represents the basic level of 100% activity
392 of the certain bacteriophage.
- 393 - For M13 bacteriophage, the activity drops 0.0068718 ± 0.0021243 pp with the increase
394 of 1 mV^2 of the squared zeta potential of the polymer.
- 395 - The activity drops 3.646578 ± 0.7646678 pp with the increase of $1 \mu\text{m}$ of the average
396 radius of the plastic microparticle.
- 397 - The activity rises 0.0581181 ± 0.013755 pp with the increase of $1 \mu\text{m}^2$ of the squared
398 average radius of the plastic microparticle.

399

400 The change of fitted value y_i depending on the *radius* is presented in **Figure S11** (*cf.*

401 **Figure S7**).



402

403 **Figure S11.** Change of the fitted y_i depending on the radius of the plastic microparticles.

404

405 **2.5. Model 2**

406 Model 2 was based on the coarse estimation, where phages were replaced by interactions
 407 between the phage type and zeta potential squared.

Source	SS	df	MS	Number of obs	=	37
Model	21932.2554	14	1566.58967	F(14, 22)	=	8.01
Residual	4301.32214	22	195.514643	Prob > F	=	0.0000
				R-squared	=	0.8360
				Adj R-squared	=	0.7317
Total	26233.5775	36	728.710487	Root MSE	=	13.983

y	Coefficient	Std. err.	t	P> t	[95% conf. interval]	
int_t4_zeta2	-.0062459	.0024041	-2.60	0.016	-.0112317	-.0012602
int_ms2_zeta2	-.0100222	.0024041	-4.17	0.000	-.015008	-.0050365
int_m13_zeta2	-.0140335	.0024041	-5.84	0.000	-.0190192	-.0090477
abs	-31.58638	13.20681	-2.39	0.026	-58.97562	-4.197135
hips	-8.059362	13.34243	-0.60	0.552	-35.72987	19.61115
pa6	-8.008128	13.98612	-0.57	0.573	-37.01356	20.9973
pc	4.15582	12.62334	0.33	0.745	-22.02339	30.33502
pe	3.165382	12.78384	0.25	0.807	-23.34668	29.67745
pet	-70.60276	14.02794	-5.03	0.000	-99.69493	-41.5106
pmma	-1.273046	13.20681	-0.10	0.924	-28.66229	26.1162
pp	-4.605286	12.14838	-0.38	0.708	-29.79948	20.58891
ps	-35.79936	13.34243	-2.68	0.014	-63.46987	-8.128851
ptfe	6.397717	12.56614	0.51	0.616	-19.66287	32.4583
pur	-19.40862	12.63479	-1.54	0.139	-45.61157	6.794334
pvc	0 (omitted)					
_cons	100	13.98266	7.15	0.000	71.00175	128.9983

408
 409 Next, the unnecessary variables were removed (i.e., those whose β coefficients might
 410 be equal to 0 due to statistical analysis). This action aimed to determine for which polymers the
 411 DLVO theory is not sufficient.

412

Source	SS	df	MS	Number of obs	=	37
Model	21317.3771	7	3045.33959	F(7, 29)	=	17.96
Residual	4916.20043	29	169.524153	Prob > F	=	0.0000
				R-squared	=	0.8126
				Adj R-squared	=	0.7674
Total	26233.5775	36	728.710487	Root MSE	=	13.02

y	Coefficient	Std. err.	t	P> t	[95% conf. interval]	
int_t4_zeta2	-.0057495	.0017333	-3.32	0.002	-.0092945	-.0022044
int_ms2_zeta2	-.0095258	.0017333	-5.50	0.000	-.0130708	-.0059807
int_m13_zeta2	-.013537	.0017333	-7.81	0.000	-.017082	-.0099919
abs	-30.21608	8.028997	-3.76	0.001	-46.63722	-13.79493
pet	-68.92525	8.191872	-8.41	0.000	-85.67951	-52.17099
ps	-34.37615	8.050589	-4.27	0.000	-50.84145	-17.91085
pur	-18.27415	7.966349	-2.29	0.029	-34.56716	-1.981135
_cons	97.62429	4.714613	20.71	0.000	87.98182	107.2668

414 ***F*-statistic, R^2 , adjusted R^2**

415 As the F-statistic is equal to 17.96 and the p-value ≈ 0.0000 , we can conclude a statistically
 416 significant relationship between y and the chosen explanatory variables. 81.26% of the variance
 417 of y is explained by the chosen explanatory variables. The adjusted R^2 (correcting the positive
 418 bias related to the number of observations and number of explanatory variables) shows that the
 419 model should explain 76.74% of the variance of y in the population.

420 ***Ramsey RESET test***

Ramsey RESET test for omitted variables
 Omitted: Powers of fitted values of y

H_0 : Model has no omitted variables

$F(3, 26) = 2.50$

421 Prob > F = 0.0820

422 With a p-value of 0.0820, we fail to reject the hypothesis of the correct specification of the
 423 model (significance level of 0.05). However, we did not fail to reject the hypothesis on the
 424 significance level of 0.10. On the significance level of 0.05, we failed to reject the
 425 hypothesis that estimated parameters are equal to zero.

426 ***Correlation Matrix***

427 There is no high collinearity between any variables.

	int_t4~2	~2_zeta2	int_m1~2	abs	pet	ps	pur
int_t4_zeta2	1.0000						
int_ms2_ze~2	-0.3139	1.0000					
int_m13_ze~2	-0.3139	-0.3139	1.0000				
abs	-0.0330	-0.0330	-0.0330	1.0000			
pet	-0.0738	-0.0738	-0.0738	-0.0882	1.0000		
ps	-0.0400	-0.0400	-0.0400	-0.0882	-0.0882	1.0000	
428 pur	-0.0017	-0.0017	-0.0017	-0.0882	-0.0882	-0.0882	1.0000

429 ***Multicollinearity***

430 VIF values are much lower than 10.

Variable	VIF	1/VIF
int_m13_ze~2	1.48	0.675259
int_ms2_ze~2	1.48	0.675259
int_t4_zeta2	1.48	0.675259
pet	1.09	0.916362
ps	1.05	0.948807
abs	1.05	0.953917
pur	1.03	0.968979
Mean VIF	1.24	

431

432 Residuals analysis and homoskedasticity

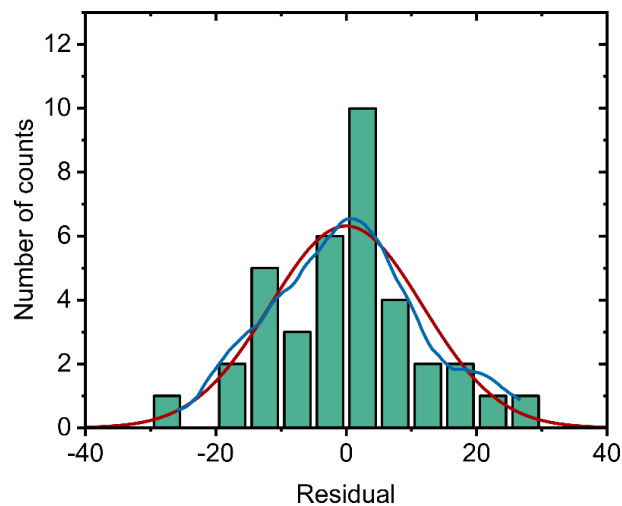
433 According to the Shapiro-Wilk test, we fail to reject the 0-hypothesis of the normal distribution
 434 of residuals in the model at the significance level of 0.05 (p-value = 0.83799). The distribution
 435 is presented in **Figure S12**. The Kernel density plot (here normalized to a number of counts)
 436 almost matches the Gaussian curve. No strong skewness or kurtosis were noticed.

Shapiro-Wilk W test for normal data

Variable	Obs	W	V	z	Prob>z
e	37	0.98323	0.624	-0.986	0.83799

437

438

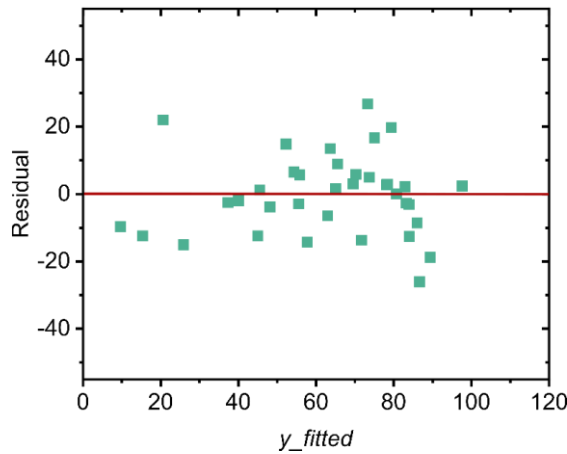


439

440 **Figure S12.** The histogram of the residuals of the model. Blue curve – Kernel density
 441 normalized to the number of counts, red curve – normal distribution.

442

443 According to the Breusch-Pagan test, we fail to reject the hypothesis of constant
 444 variance (homoskedasticity) at the significance level of 0.05. The same conclusion we received
 445 from White's test. At the same significance level, we also fail to reject the hypothesis of
 446 skewness and kurtosis of the distribution of residuals (**Figure S13**).



447

448 **Figure S13.** Residuals of the model for fitted values of y_i .

Breusch-Pagan/Cook-Weisberg test for heteroskedasticity
 Assumption: Normal error terms
 Variable: Fitted values of y

H0: Constant variance

chi2(1) = 0.14
 Prob > chi2 = 0.7054

449

White's test
 H0: Homoskedasticity
 Ha: Unrestricted heteroskedasticity

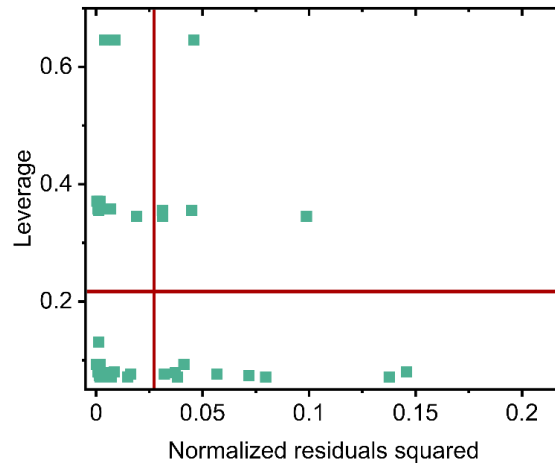
chi2(18) = 10.01
 Prob > chi2 = 0.9315

Cameron & Trivedi's decomposition of IM-test

Source	chi2	df	p
Heteroskedasticity	10.01	18	0.9315
Skewness	6.25	7	0.5107
Kurtosis	0.07	1	0.7855
Total	16.34	26	0.9277

450

451 No observations should be removed from the model because none of them was spotted in the
 452 upper-right corner of the leverage-normalized residuals squared plot (**Figure S14**). In other
 453 words, there is no observation that strongly bios the estimated β -coefficients.



454
 455 **Figure S14.** The leverages-normalized residual squared analysis.

456
 457 To prove it, the observation visible in the middle of the graph was removed. The model
 458 B – building was repeated, leading to the same form of the model.

Source	SS	df	MS	Number of obs	=	36
Model	20918.7871	7	2988.39815	F(7, 28)	=	17.02
Residual	4916.19373	28	175.578348	Prob > F	=	0.0000
				R-squared	=	0.8097
				Adj R-squared	=	0.7621
Total	25834.9808	35	738.142309	Root MSE	=	13.251

y	Coefficient	Std. err.	t	P> t	[95% conf. interval]
int_t4_zeta2	-.0057511	.0017851	-3.22	0.003	-.0094078 -.0020945
int_ms2_zeta2	-.0095251	.0017668	-5.39	0.000	-.0131443 -.0059059
int_m13_zeta2	-.0135363	.0017668	-7.66	0.000	-.0171556 -.0099171
abs	-30.21276	8.188771	-3.69	0.001	-46.98669 -13.43882
pet	-68.92203	8.353212	-8.25	0.000	-86.03281 -51.81125
ps	-34.37285	8.210527	-4.19	0.000	-51.19135 -17.55435
pur	-18.27076	8.125935	-2.25	0.033	-34.91598 -1.625533
_cons	97.62128	4.82278	20.24	0.000	87.74226 107.5003

459
 460 This operation resulted in a minuscule decrease in the standard errors of the coefficients.
 461 It also decreased the R^2 .

462
 463

464 **Interpretation of the model:**

465 According to the diagnostics, the model seems valid for drawing nonbiased conclusions on the
466 described phenomenon. However, it is essential to mention that the model was based only on
467 36 experiments (each experiment consisted of 3 repetitions of 8 repetitions of the phage
468 titration) and the additional theoretical observation (base 100% activity of the specific
469 bacteriophage after 24 h if any polymer was added). Due to so few observations, the model may
470 omit some important information, even if the statistical analysis based on the available data is
471 valid. This issue is also visible in relatively high standard errors of the estimated parameters.

472 The final form of the model assumes independent variables and their impact on the
473 explained variable y_i (the activity of the bacteriophage after 24 h [%]):

$$474 \quad y_i = \beta_0 + \beta_1 \cdot \text{int_t4_zeta2} + \beta_2 \cdot \text{int_ms2_zeta2} + \beta_3 \cdot \text{int_m13_zeta2} + \beta_4 \cdot \text{abs} + \beta_5 \cdot \\ 475 \quad \text{pet} + \beta_6 \cdot \text{ps} + \beta_7 \cdot \text{pur} \quad (12)$$

476 81.26% of the variance of y is explained by the chosen explanatory variables. The
477 adjusted R^2 (correcting the positive bias related to the number of observations and number of
478 explanatory variables) shows that the model should explain 76.74% of the variance of y in the
479 population. The model's estimated parameters (coefficients) are given in **Table S4**.

480

481 **Table S4.** Estimated parameters (coefficients) of the model.

Estimated parameter	Value	Standard Error	Unit
β_0	97.62429	4.714613	-
β_1	-0.0057495	0.0017333	mV ⁻²
β_2	-0.0095258	0.0017333	mV ⁻²
β_3	-0.0135370	0.0017333	mV ⁻²
β_4	-30.21608	8.028997	-
β_5	-68.92525	8.191872	-
β_6	-34.37615	8.050589	-
β_7	-18.27415	7.966349	-

482

483 - The constant value $\beta_0 = 97.62429 \pm 4.714613$ represents the basic level of 100% activity
 484 of the specific bacteriophage.

485 - For T4 bacteriophage, the activity drops 0.0057495 ± 0.0017333 pp with the increase of
 486 1 mV² of the squared zeta potential of the polymer.

487 - For MS2 bacteriophage, the activity drops 0.0095258 ± 0.0017333 pp with the increase
 488 of 1 mV² of the squared zeta potential of the polymer.

489 - For M13 bacteriophage, the activity drops 0.0135370 ± 0.0017333 pp with the increase
 490 of 1 mV² of the squared zeta potential of the polymer.

491 - The activity drops 30.21608 ± 8.028997 pp if in the experiment ABS was used.

492 - The activity drops 68.92525 ± 8.191872 pp if in the experiment PET was used.

493 - The activity drops 34.37615 ± 8.050589 pp if in the experiment PS was used.

494 - The activity drops 18.27415 ± 7.966349 pp if in the experiment PUR was used.

495

496 This model shows that the activity of the bacteriophage suspension can be explained by
497 the interaction between the type of the phage and the zeta potential of the polymer. It is
498 sufficient for most polymers except for ABS, PET, PS, and PUR, which, if present, decreases
499 the activity of the bacteriophage suspension.
500

501 **References**

- 502 Armanious, A., M. Aeppli, R. Jacak, D. Refardt, T. Sigstam, et al. 2016. Viruses at Solid-
503 Water Interfaces: A Systematic Assessment of Interactions Driving Adsorption. *Environ.*
504 *Sci. Technol.* 50(2): 732–743. doi: 10.1021/acs.est.5b04644.
- 505 Derjaguin, B. V., N. V. Churaev, and V.M. Muller. 1987. The Derjaguin—Landau—
506 Verwey—Overbeek (DLVO) Theory of Stability of Lyophobic Colloids. *Surface Forces.*
507 Springer US, Boston, MA. p. 293–310
- 508 Greve, J., and J. Blok. 1975. Transient electric birefringence of T-even bacteriophages. II.
509 T4B in the Presence of tryptophan and T4D. *Biopolymers* 14(1): 139–154. doi:
510 10.1002/bip.1975.360140111.
- 511 Hosseinidoust, Z., T.G.M. Van De Ven, and N. Tufenkji. 2011. Bacterial capture efficiency
512 and antimicrobial activity of phage-functionalized model surfaces. *Langmuir* 27(9):
513 5472–5480. doi: 10.1021/la200102z.
- 514 Kolska, Z., Z. Makajova, K. Kolarova, N. Kasalkova, S. Trostova, et al. 2013. Electrokinetic
515 Potential and Other Surface Properties of Polymer Foils and Their Modifications. *Polym.*
516 *Sci.* (iv). doi: 10.5772/46144.
- 517 Kuzmanovic, D.A., I. Elashvili, C. Wick, C. O’Connell, and S. Krueger. 2003. Bacteriophage
518 MS2: molecular weight and spatial distribution of the protein and RNA components by
519 small-angle neutron scattering and virus counting. *Structure* 11(11): 1339–1348. doi:
520 10.1016/j.str.2003.09.021.
- 521 Leiman, P.G., F. Arisaka, M.J. Van Raaij, V.A. Kostyuchenko, A.A. Aksyuk, et al. 2010.
522 Morphogenesis of the T4 tail and tail fibers. *Viol. J.* 7: 1–28. doi: 10.1186/1743-422X-
523 7-355.
- 524 Moghimian, P., V. Srot, B.P. Pichon, S.J. Facey, and P.A. van Aken. 2016. Stability of M13
525 Phage in Organic Solvents. *J. Biomater. Nanobiotechnol.* 7(2): 72–77. doi:
526 10.4236/jbnb.2016.72009.
- 527 Mycielski, J. 2010. *Ekonometria.* Uniwersytet Warszawski. Wydział Nauk Ekonomicznych,
528 Warsaw.
- 529 Ohshima, H. 2012. The Derjaguin-Landau-Verwey-Overbeek (DLVO) Theory of Colloid
530 Stability. *Electrical Phenomena at Interfaces and Biointerfaces.* John Wiley & Sons, Inc.,
531 Hoboken, NJ, USA. p. 27–34
532 polymerdatabase.com.
- 533 Putra, B.R., K. Szot-Karpińska, P. Kudła, H. Yin, J.A. Boswell, et al. 2019. Bacteriophage
534 M13 Aggregation on a Microhole Poly(ethylene terephthalate) Substrate Produces an
535 Anionic Current Rectifier: Sensitivity toward Anionic versus Cationic Guests. *ACS*
536 *Appl. Bio Mater.* 3(1): 512–521. doi: 10.1021/ACSABM.9B00952.
- 537 Schrader, M.E. 1995. Young-Dupre Revisited. *Langmuir* 11(9): 3585–3589. doi:
538 10.1021/la00009a049.
- 539 Thommes, M., K. Kaneko, A. V. Neimark, J.P. Olivier, F. Rodriguez-Reinoso, et al. 2015.
540 Physisorption of gases, with special reference to the evaluation of surface area and pore
541 size distribution (IUPAC Technical Report). *Pure Appl. Chem.* 87(9–10): 1051–1069.
542 doi: 10.1515/pac-2014-1117.
- 543 Yap, M.L., and M.G. Rossmann. 2014. Structure and function of bacteriophage T4. *Future*
544 *Microbiol.* 9(12): 1319–1337. doi: 10.2217/fmb.14.91.
545